




## ORIGINAL ARTICLE

# Protease-activated receptor-2 accelerates intestinal tumor formation through activation of nuclear factor- $\kappa$ B signaling and tumor angiogenesis in *Apc*<sup>Min/+</sup> mice

Makiko Kawaguchi<sup>1</sup>  | Koji Yamamoto<sup>1</sup> | Hiroaki Kataoka<sup>1</sup>  | Aya Izumi<sup>1</sup> | Fumiki Yamashita<sup>1</sup> | Takumi Kiwaki<sup>1</sup> | Takahiro Nishida<sup>1</sup> | Eric Camerer<sup>2</sup> | Tsuyoshi Fukushima<sup>1</sup> 

<sup>1</sup>Department of Pathology, University of Miyazaki, Miyazaki, Japan

<sup>2</sup>Inserm U970, Paris Cardiovascular Research Center, Université de Paris, Paris, France

## Correspondence

Tsuyoshi Fukushima, Section of Oncopathology and Regenerative Biology, Department of Pathology, Faculty of Medicine, University of Miyazaki, Miyazaki, Japan.  
Email: fukuchan@med.miyazaki-u.ac.jp

## Funding information

Japan Society for the Promotion of Science KAKENHI, Grant/Award Number: 15K08311, 16H05175 and 17K08764; Agence Nationale de la Recherche, Grant/Award Number: ANR-15-CE14-0009

## Abstract

Hepatocyte growth factor activator inhibitor-1 (HAI-1), encoded by the *SPINT1* gene, is a membrane-bound protease inhibitor expressed on the surface of epithelial cells. Hepatocyte growth factor activator inhibitor-1 regulates type II transmembrane serine proteases that activate protease-activated receptor-2 (PAR-2). We previously reported that deletion of *Spint1* in *Apc*<sup>Min/+</sup> mice resulted in accelerated formation of intestinal tumors, possibly through enhanced nuclear factor- $\kappa$ B signaling. In this study, we examined the role of PAR-2 in accelerating tumor formation in the *Apc*<sup>Min/+</sup> model in the presence or absence of *Spint1*. We observed that knockout of the *F2r1* gene, encoding PAR-2, not only eliminated the enhanced formation of intestinal tumors caused by *Spint1* deletion, but also reduced tumor formation in the presence of *Spint1*. Exacerbation of anemia and weight loss associated with HAI-1 deficiency was also normalized by compound deficiency of PAR-2. Mechanistically, signaling triggered by deregulated protease activities increased nuclear translocation of RelA/p65, vascular endothelial growth factor expression, and vascular density in *Apc*<sup>Min/+</sup>-induced intestinal tumors. These results suggest that serine proteases promote intestinal carcinogenesis through activation of PAR-2, and that HAI-1 plays a critical tumor suppressor role as an inhibitor of matriptase, kallikreins, and other PAR-2 activating proteases.

## KEYWORDS

angiogenesis, colon cancer, HAI-1, PAR-2, *Spint1*

## 1 | INTRODUCTION

Hepatocyte growth factor activator inhibitor-1 (HAI-1)/serine peptidase inhibitor, Kunitz type 1 (*SPINT1*), encoded by the human *SPINT1*

gene, is a membrane-associated Kunitz-type serine protease inhibitor that is expressed by most epithelial cells and placental cytotrophoblasts.<sup>1</sup> It was initially identified as a cellular inhibitor of serum hepatocyte growth factor and subsequent studies have indicated that HAI-1 is also a critical regulator of epithelial type II

This is an open access article under the terms of the Creative Commons Attribution-NonCommercial License, which permits use, distribution and reproduction in any medium, provided the original work is properly cited and is not used for commercial purposes.

© 2020 The Authors. *Cancer Science* published by John Wiley & Sons Australia, Ltd on behalf of Japanese Cancer Association.

transmembrane serine proteases (TTSPs), particularly matriptase.<sup>2,3</sup> Previously, we generated several *Spint1* mutant mouse models and showed that HAI-1 contributes to the integrity of epithelia, including the intestinal epithelium.<sup>2,4</sup> Intestine-specific *Spint1* knockout mice showed increased susceptibility to dextran sulfate sodium-induced experimental colitis.<sup>4</sup> Moreover, the *Spint1* deletion led to accelerated tumor formation in the *Apc*<sup>Min/+</sup> mouse model, indicating that HAI-1 is a tumor suppressor.<sup>5</sup> Indeed, the cell surface immunoreactivity of HAI-1 was markedly reduced in carcinoma cells compared to adjacent normal enterocytes or adenoma cells in human colon cancers,<sup>6,7</sup> and this trend was confirmed in a murine *Apc*<sup>Min/+</sup> model.<sup>5</sup> Consequently, the ratio of HAI-1 expression relative to its target epithelial protease, matriptase, was decreased along with the progression of colon cancers.<sup>8</sup> Enhanced tumor formation observed in HAI-1-deficient *Apc*<sup>Min/+</sup> mice was mediated, at least partly, by activation of nuclear factor (NF)- $\kappa$ B signaling<sup>9</sup>; however, detailed mechanisms underlying NF- $\kappa$ B activation in the absence of HAI-1 remain unclear.

Protease-activated receptor-2 (PAR-2) is a 7 transmembrane-spanning domain G protein-coupled receptor widely expressed by epithelial, endothelial, and smooth muscle cells, with diverse physiological and pathological functions.<sup>10-13</sup> Specific cleavage by trypsin-like serine proteases frees an endogenous ligand for interaction with the core of the receptor, inducing a conformational change that triggers signal transduction.<sup>10,14,15</sup> Type II transmembrane serine proteases are known to activate PAR-2<sup>16-21</sup> and PAR-2 reportedly contributes to tumor progression through its promotion of invasive growth by cancer cells and by stimulating angiogenesis.<sup>11,19,22</sup> Among TTSPs, matriptase is the most potent PAR-2 activator known in epithelial and tumor tissues.<sup>22,23</sup> Transgenic expression of matriptase in murine keratinocytes induces skin carcinogenesis<sup>24</sup> that is entirely dependent on PAR-2 signaling.<sup>25</sup> Activation of PAR-2 by transgenic matriptase expression led to protumorigenic cytokine expression through activation of NF- $\kappa$ B signaling.<sup>25</sup> Previously, we reported that the loss of intestinal HAI-1/*Spint1* led to increased trypsin-like serine protease activity in *Apc*<sup>Min/+</sup> mouse intestine.<sup>9</sup> We thus hypothesize that HAI-1 insufficiency permits the unrestricted activity of pericellular trypsin-like serine proteases, including matriptase, leading to activation of PAR-2/NF- $\kappa$ B signaling in colon cancer tissues.

To test this hypothesis, we generated *Apc*<sup>Min/+</sup> mice with an intestine-specific *Spint1*-deletion with or without the superimposition of global PAR-2/*F2rl1* deletion to analyze the effects of PAR-2 signaling on intestinal carcinogenesis and on the enhanced tumor susceptibility induced by HAI-1 deficiency. We found that the deletion of *F2rl1* reduced tumor formation both in control and *Spint1*-deleted *Apc*<sup>Min/+</sup> mice and decreased the activation of NF- $\kappa$ B and angiogenesis in HAI-1 deficient tumors.

## 2 | MATERIALS AND METHODS

### 2.1 | Mice

All animal experiments were carried out using protocols approved by the Institutional Animal Care and Use Committee of the University

of Miyazaki. *Apc*<sup>Min/+</sup> mice and *Villin-Cre* mice were obtained from The Jackson Laboratory. *Apc*<sup>Min/+</sup> *Spint1*<sup>LoxP/LoxP/Villin-Cre</sup> mice<sup>4,5</sup> were crossed with *F2rl1*-deficient mice<sup>26</sup> to generate *Apc*<sup>Min/+</sup> mice with an intestine-specific *Spint1* deletion and global PAR-2/*F2rl1* deletion (*Spint1*<sup>LoxP/LoxP/Villin-Cre/F2rl1<sup>-/-</sup>/Apc<sup>Min/+</sup>). Mice were assessed daily, and body weights were recorded weekly. Blood samples were obtained from the right ventricle, and EDTA-containing plasma samples were used for analyzing hemoglobin concentration.</sup>

At 15 weeks of age, all mice were killed to evaluate the number and sizes of intestinal tumors. The tumor size was scored as previously described.<sup>5</sup> For histological analysis, intestinal tissues were fixed in 4% paraformaldehyde in PBS and embedded in paraffin. Four-micrometer-thick sections were stained with H&E or processed for immunohistochemical analysis.

### 2.2 | Quantitative RT-PCR

Total RNA was prepared with TRIzol (Life Technologies Japan), followed by DNase I (Takara Bio) treatment. For RT-PCR, 3  $\mu$ g total RNA was reverse-transcribed with a mixture of Oligo (dT)12-18 (Life Technologies Japan) and random primers (6 mers) (Takara Bio) using 200 units of ReverTra Ace (Toyobo), and 1/30 of the resulting cDNA was processed for quantitative RT-PCR. Real-time RT-PCR was undertaken in a Thermal Cycler Dice Real Time System II (Takara Bio) using the SYBR Premix Ex Taq II (Takara Bio). For internal control,  $\beta$ -actin mRNA was also measured. The following primers were used:  $\beta$ -actin forward, 5'-TGACAGGATGCAGAAGGAGA, and reverse, 5'-GC TGGAAAGGTGGACAGTGAG; *Pecam1* (CD31) forward, 5'-GGAA GCCAACAGCCATTACGG, and reverse, 5'-GAGCCTCCGTTCT CTTGGTGA; *Vegfa* forward, 5'-CAGGCTGCTGAACGATGAA, and reverse, 5'-CTGCATTCACATCTGCTGTG; *Bcl2* (Bcl-2) forward, 5'-ACCGTCGTGACTTCGCAGAG, and reverse, 5'-GGTGTGCAG ATGCCGGTTCA; and *Bad* forward, 5'-GCCCTAGGCTTGAGGAAGTC, and reverse, 5'-CAAACCTCTGGGATCTGGAACA.

### 2.3 | Immunohistochemical analyses

For immunohistochemistry, tissue sections were processed for antigen retrieval by microwaving for 10 minutes at 96°C in 10 mmol/L citrate buffer (pH 6.0), followed by treatment with 3% H<sub>2</sub>O<sub>2</sub> in PBS for 10 minutes. After blocking in 5% normal goat serum (Dako) in PBS, the sections were incubated with anti-NF- $\kappa$ B p65 (RelA/p65) rabbit mAb (Cell Signaling Technology) or anti-CD31 rabbit polyclonal Ab (Cell Signaling Technology), or antiphosphorylated MET (Y1235) rabbit polyclonal Ab,<sup>27</sup> or anti- $\beta$ -catenin rabbit polyclonal Ab (Sigma-Aldrich) or anti-CD45 rat mAb (Wuxi Biosciences) for 16 hours at 4°C and then incubated with Envision labeled polymer reagents (Dako) for 30 minutes at room temperature. The reactions were revealed by nickel and cobalt-3,3'-diaminobenzidine (Pierce) and counterstained with Mayer's hematoxylin. To quantify RelA/p65 nuclear translocation and CD31<sup>+</sup> vessels, stained sections with

nonneoplastic mucosa and tumor tissues were selected and photographed at 200× magnification. Two independent investigators counted the RelA/p65<sup>+</sup> nuclei and CD31<sup>+</sup> vessels and the mean number per field was calculated. To evaluate the immunoreactivity of phosphorylated MET, we scored as described by Fukushima et al.<sup>27</sup>

## 2.4 | Cell culture

The Caco2 cell line was obtained from the Riken BRC Cell Bank. Cells were cultured in DMEM containing 10% FBS. For transient silencing of *F2RL1*, 2 kinds of siRNA were used. One (PAR-2 siRNA #1) was an siRNA pool (ON-TARGETplus SMARTpool siRNA; Thermo Fisher Scientific) used with the siGENOME Non-Targeting siRNA pool as a control. The other (PAR-2 siRNA #2) was Stealth siRNA (Invitrogen) and the sequence was 5'-UCAACCACUGUUAAGACCUCCUAUU-3'. Transfection was carried out using Lipofectamine RNAiMax reagent (Invitrogen) followed by cultivation in DMEM supplemented with 10% FBS for 24 hours. The cells were treated with or without 10 μmol/L PAR-2 agonist, Ser-Leu-Ile-Gly-Arg (SLIGR)-NH<sub>2</sub>, or 10 μmol/L PAR-2 selective antagonist, Phe-Ser-Leu-Leu-Arg-Tyr (FSLRY)-NH<sub>2</sub> (Peptides International).<sup>28</sup>

## 2.5 | Immunoblot analysis

Mouse intestinal tumors were homogenized on ice in CelLytic MT (Sigma-Aldrich) supplemented with protease inhibitor cocktail (Sigma-Aldrich), 100 mmol/L NaF, and 1 mmol/L Na<sub>3</sub>VO<sub>4</sub>. The extracts were centrifuged at 20 000 g for 15 minutes at 4°C, and the resulting supernatants were used for experiments. Cellular proteins were extracted with CelLytic M (Sigma-Aldrich) supplemented with protease inhibitor cocktail, 100 mmol/L NaF, and 1 mmol/L Na<sub>3</sub>VO<sub>4</sub>, centrifuged 15 000 g for 15 minutes, and the supernatants were collected. Equal amounts of total proteins were separated by SDS-PAGE under reducing conditions using 4%-12% gradient gels and transferred onto an Immobilon-P membrane (Millipore). After blocking with 5% nonfat milk in 25 mmol/L TBS with 0.1% Tween-20, pH 7.6 (TBS-T), the membranes were incubated overnight at 4°C with primary Ab, followed by washing with TBS-T and incubation with HRP-conjugated secondary Ab diluted in TBS-T with 1% BSA for 1 hour at room temperature. The labeled proteins were visualized with a chemiluminescence reagent (PerkinElmer Life Science). The following primary Abs were used: anti-β-actin mouse mAb (Sigma-Aldrich), anti-PAR-2 rabbit mAb, anti-phospho-NF-κB p65 (Ser536) rabbit mAb and anti-NF-κB p65 rabbit mAb (Cell Signaling Technology Japan).

## 2.6 | Enzyme-linked immunosorbent assay

Serum vascular endothelial growth factor (VEGF)-A levels of mice and human VEGF-A levels in culture supernatants of Caco2 were

measured with a Quantikine VEGF ELISA kit (R&D Systems) according to the manufacturer's instructions.

## 2.7 | Statistical analysis

Statistical analysis was carried out using StatView 5.0 (SAS). Comparison between 2 unpaired groups was made with repeated-measure of variance or the Mann-Whitney *U* test. Significance was set at *P* < .05.

## 3 | RESULTS

### 3.1 | Deficiency in PAR-2 alleviates increased tumor formation in *Spint1*-deleted *Apc*<sup>Min/+</sup> mice

Consistent with the previously reported increase in tumor burden,<sup>5</sup> *Spint1*-deleted *Apc*<sup>Min/+</sup> (*Spint1*<sup>LoxP/LoxP</sup>/*Villin-Cre/Apc*<sup>Min/+</sup>) mice gained significantly less weight with age than *Apc*<sup>Min/+</sup> control mice. Strikingly, this phenotype was completely reversed by concomitant deletion of *F2rl1* (*Spint1*<sup>LoxP/LoxP</sup>/*Villin-Cre/F2rl1*<sup>-/-</sup>/*Apc*<sup>Min/+</sup>; Figure 1A). Profound anemia of *Spint1*-deleted *Apc*<sup>Min/+</sup> mice was also normalized to *Apc*<sup>Min/+</sup> control levels with compound PAR-2 deficiency, although hematocrits remained lower than in naïve mice (Figure 1B). Fifteen weeks after birth, the number of intestinal tumors was significantly (*P* = .0001) increased in *Spint1*<sup>LoxP/LoxP</sup>/*Villin-Cre/Apc*<sup>Min/+</sup> (146.6 ± 4.5, *n* = 10) compared with control *Spint1*<sup>LoxP/LoxP</sup>/*Apc*<sup>Min/+</sup> mice (85.4 ± 5.7, *n* = 11) (Figure 2A,B). Again, concomitant deletion of *F2rl1* in *Spint1*<sup>LoxP/LoxP</sup>/*Villin-Cre/Apc*<sup>Min/+</sup> mice significantly (*P* = .0003) reduced the number of intestinal tumors (92.9 ± 7.3, *n* = 11) (Figure 2B). Intriguingly, deletion of *F2rl1* also reduced the number of tumors formed in *Apc*<sup>Min/+</sup> mice in the presence of *Spint1* (*Spint1*<sup>LoxP/LoxP</sup>/*F2rl1*<sup>-/-</sup>/*Apc*<sup>Min/+</sup>) (*P* = .0486). *F2rl1* deletion also significantly decreased the size of tumors in both the control (*P* = .0046) and *Spint1*<sup>LoxP/LoxP</sup>/*Villin-Cre/Apc*<sup>Min/+</sup> mice (*P* = .0092) (Figures 2B and S1). However, tumor histology was not visibly altered by the deletion of *F2rl1* (Figure 2C).

### 3.2 | Protease-activated receptor-2 drives NF-κB activation induced by *Spint1* deletion

We previously reported that NF-κB signaling is activated in HAI-1-deficient *Apc*<sup>Min/+</sup> tumors. Moreover, an NF-κB inhibitor suppressed the HAI-1 loss-mediated enhancement of tumorigenicity in *Apc*<sup>Min/+</sup> mice.<sup>9</sup> Protease-activated receptor-2 is known to activate NF-κB signaling in various human cancers, including colon cancer,<sup>25,29-31</sup> and HAI-1 regulates PAR-2-activating TTSPs.<sup>22</sup> Thus, the activation of NF-κB in HAI-1-deficient intestine might result from the excessive activation of PAR-2. To test this hypothesis, we evaluated the effect of *F2rl1* deletion on the nuclear translocation of the NF-κB subunit RelA/p65. The

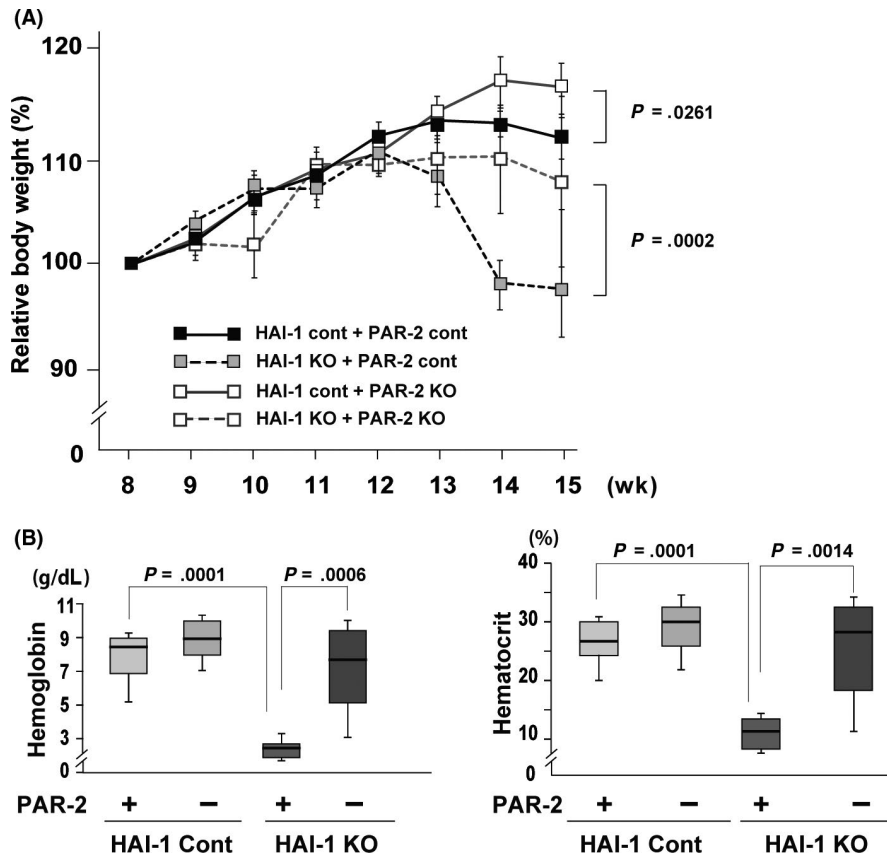


**FIGURE 1** Protease-activated receptor-2 (PAR-2) deficiency improved the health of *Apc*<sup>Min/+</sup> mice deficient in intestinal hepatocyte growth factor activator inhibitor-1 (HAI-1). A, Relative body weight (mean ± SEM) of *Spint1*<sup>LoxP/LoxP</sup>/*Apc*<sup>Min/+</sup> mice (HAI-1 control [cont] + PAR-2 cont) (n = 11), *Spint1*<sup>LoxP/LoxP</sup>/*F2r1*<sup>-/-</sup>/*Apc*<sup>Min/+</sup> mice (HAI-1 cont + PAR-2 knockout [KO]) (n = 11), *Spint1*<sup>LoxP/LoxP</sup>/*Villin-Cre/Apc*<sup>Min/+</sup> mice (HAI-1 KO + PAR-2 cont) (n = 10), and *Spint1*<sup>LoxP/LoxP</sup>/*Villin-Cre/F2r1*<sup>-/-</sup>/*Apc*<sup>Min/+</sup> mice (HAI-1 KO + PAR-2 KO) (n = 11). B, Mean hemoglobin concentration (left panel) and hematocrit levels (right panel) of the mice. Box and whiskers indicate the interquartile range and sample maxima and minima, respectively. Median is indicated by a bold line

ablation of PAR-2/*F2r1* abrogated the enhanced nuclear translocation (Figure 3A,B) and phosphorylation of RelA/p65 resulting from the loss of HAI-1 (Figure 3C) in intestinal tumors. The enhanced nuclear translocation of RelA/p65 was also observed in stroma cells adjacent to the tumor cells in HAI-1-deficient intestine, which was alleviated by the concomitant deletion of *F2r1* (Figure S2A). To support this, the number of CD45<sup>+</sup> cells increased in the HAI-1-deficient intestine (Figure S2B). These results indicate that increased NF-κB activation in *Spint1*-deleted *Apc*<sup>Min/+</sup> mice is driven by PAR-2 signaling.

### 3.3 | Protease-activated receptor-2 signaling increases VEGF-A expression and vascular density

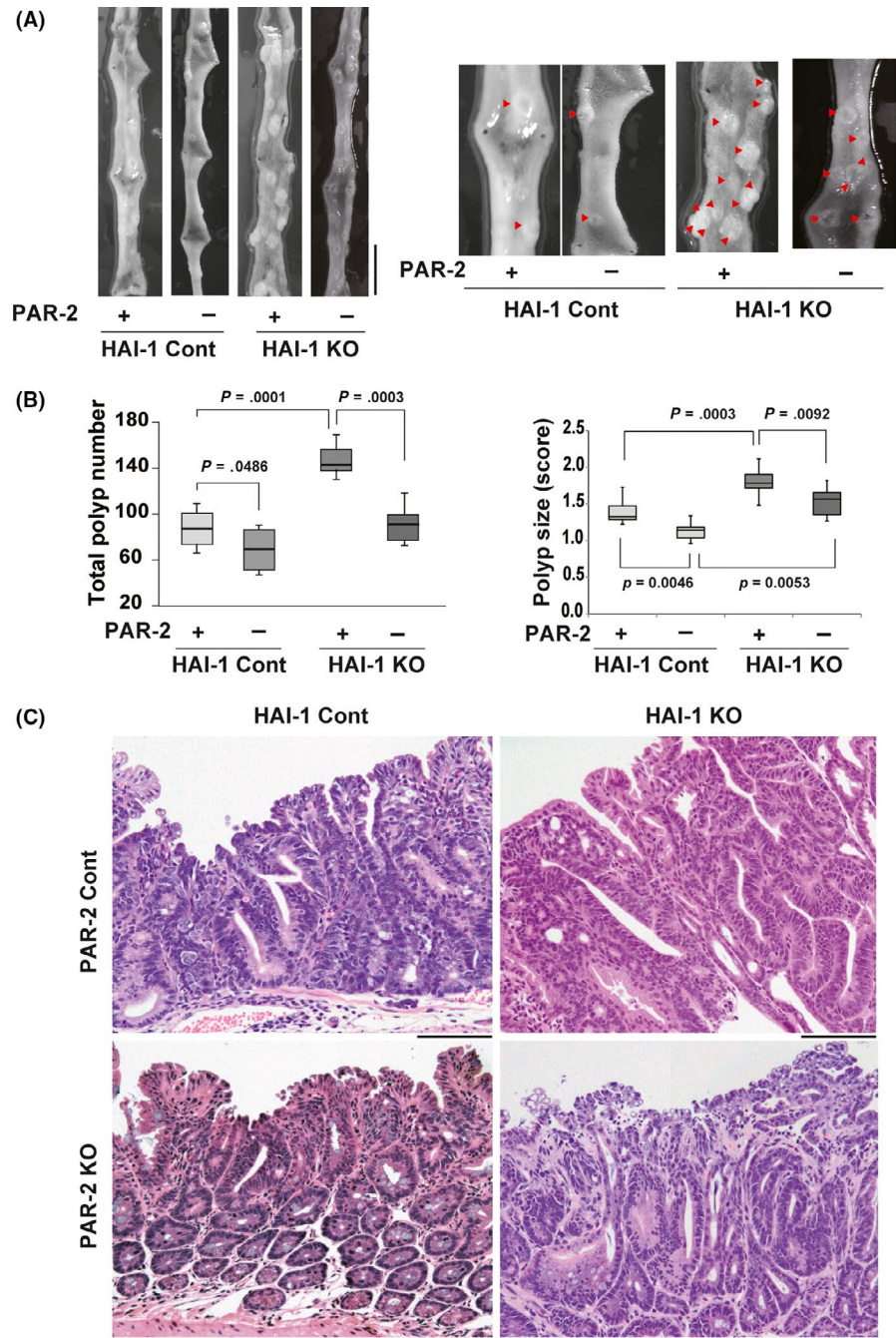
Next, we explored the mechanism by which PAR-2/NF-κB signaling increased mean intestinal tumor size and number in *Apc*<sup>Min/+</sup> mice. Protease-activated receptor-2 deficiency did not affect the Ki-67 labelling index or mRNA levels of *Bcl2* and *Bad* genes in the intestinal tumors (Figure S3), indicating that cell proliferation rate and apoptotic signals were not altered. We then examined the expression of VEGF-A, a key regulator of angiogenesis, in mouse tissues and serum. Intriguingly, there was a highly significant increase in serum VEGF-A protein levels in *Spint1*<sup>LoxP/LoxP</sup>/*Villin-Cre/Apc*<sup>Min/+</sup> mice that was abolished with compound deficiency of PAR-2 (Figure 4A). Accordingly, HAI-1 deficiency was associated with a nonsignificant increase in *Vegfa* gene expression in the *Apc*<sup>Min/+</sup> tumors that was significantly ( $P = .035$ ) decreased with the compound deficiency of PAR-2 (Figure 4B).

Consistent with PAR-2-dependent VEGF expression, capillary density was significantly ( $P = .0282$ ) decreased in tumors from *Spint1*<sup>LoxP/LoxP</sup>/*Villin-Cre/F2r1*<sup>-/-</sup>/*Apc*<sup>Min/+</sup> compared with those from *Spint1*<sup>LoxP/LoxP</sup>/*Villin-Cre/Apc*<sup>Min/+</sup> mice, although *Spint1* deficiency did not by itself significantly increase vascular density in tumors or adjacent mucosa (Figure 5A). Quantitative RT-PCR confirmed decreased mRNA levels for the *Pecam1* gene, which encodes the endothelial marker CD31, after *F2r1* deletion in both tumors and adjacent mucosa (Figure 5B). These results suggest a PAR-2-dependent effect of local HAI-1 deficiency on local and systemic VEGF-A levels that in turn impacts vascular density and tumor growth.

### 3.4 | Protease-activated receptor-2 signaling activates NF-κB signaling and enhances VEGF-A expression in Caco2 human colon cancer cell line

Finally, to examine the role of PAR-2 in NF-κB activation and VEGF-A expression of colon cancer cells, we analyzed the effects of *F2RL1* silencing, PAR-2 antagonist, or PAR-2 agonist on the Caco2 human colon carcinoma cell line. Knockdown of *F2RL1* or treatment of the cells with PAR-2 antagonist suppressed the phosphorylation of RelA/p65 (Figure 6A). In contrast, PAR-2 agonist enhanced the phosphorylation of RelA/p65 (Figure 6A). Next, we examined the effects of PAR-2 agonist and antagonist on the VEGF-A expression by Caco2 cells. As shown in Figure 6B, incubation of the cells with PAR-2 agonist enhanced VEGF-A mRNA levels. On the contrary,

**FIGURE 2** Effect of protease-activated receptor-2 (PAR-2)/*F2r1* deletion on intestinal tumor formation in *Apc*<sup>Min/+</sup> mice. A, Representative macroscopic appearance of the proximal small intestine from *Spint1*<sup>LoxP/LoxP</sup>/*Apc*<sup>Min/+</sup> mice (hepatocyte growth factor activator inhibitor-1 [HAI-1] control [cont] + PAR-2 cont) (n = 11), *Spint1*<sup>LoxP/LoxP</sup>/*F2r1*<sup>-/-</sup>/*Apc*<sup>Min/+</sup> mice (HAI-1 cont + PAR-2 knockout [KO]) (n = 11), *Spint1*<sup>LoxP/LoxP</sup>/*Villin-Cre/Apc*<sup>Min/+</sup> mice (HAI-1 KO + PAR-2 cont) (n = 10), and *Spint1*<sup>LoxP/LoxP</sup>/*Villin-Cre/F2r1*<sup>-/-</sup>/*Apc*<sup>Min/+</sup> mice (HAI-1 KO + PAR-2 KO) (n = 11). Higher magnification photographs are also shown (right panel). Arrowheads indicate neoplastic polyps. Bar = 1 cm. B, Number of intestinal polyps (mean ± SEM; left panel) and polyp size scores of the mice (right panel). Box and whiskers indicate the interquartile range and sample maxima and minima, respectively. Median is indicated by a bold line. C, Histology of tumors (H&E stain). Bar = 100 μm



PAR-2 antagonist suppressed the VEGF-A expression. The released VEGF-A proteins tended to be increased by the PAR-2 agonist treatment, but the difference was not statistically significant (Figure 6B).

## 4 | DISCUSSION

In this study, we show that ablation of PAR-2/*F2r1* nearly eliminates the enhancement of NF-κB signaling and tumor formation caused by the loss of HAI-1/*Spint1* in *Apc*<sup>Min/+</sup> mice, providing evidence that PAR-2 is critically involved in NF-κB activation and the susceptibility to carcinogenesis caused by HAI-1 insufficiency. The significance of PAR-2 on NF-κB signaling was also confirmed in the Caco2 human

colon carcinoma cell line. Protease-activated receptor-2 deficiency also reduced tumor size and number, even in the presence of *Spint1*. These results suggest that protease signaling is also spontaneously deregulated in the *Apc*<sup>Min</sup> model, contributing significantly to tumor growth.

The detailed molecular mechanisms linking activated NF-κB signaling to enhanced tumor formation remain unclear. Protease-activated receptor-2-dependent VEGF-A expression and angiogenesis induced by HAI-1 deficiency could play a role. However, it remains to be determined whether the increased VEGF-A level in *Spint1*<sup>LoxP/LoxP</sup>/*Villin-Cre/Apc*<sup>Min/+</sup> mice was a direct effect of HAI-1 deficiency-induced PAR-2 activation or an epiphenomenon of the increased tumor burden. In this regard, the mean tumor size in *Spint1*<sup>LoxP/LoxP</sup>/

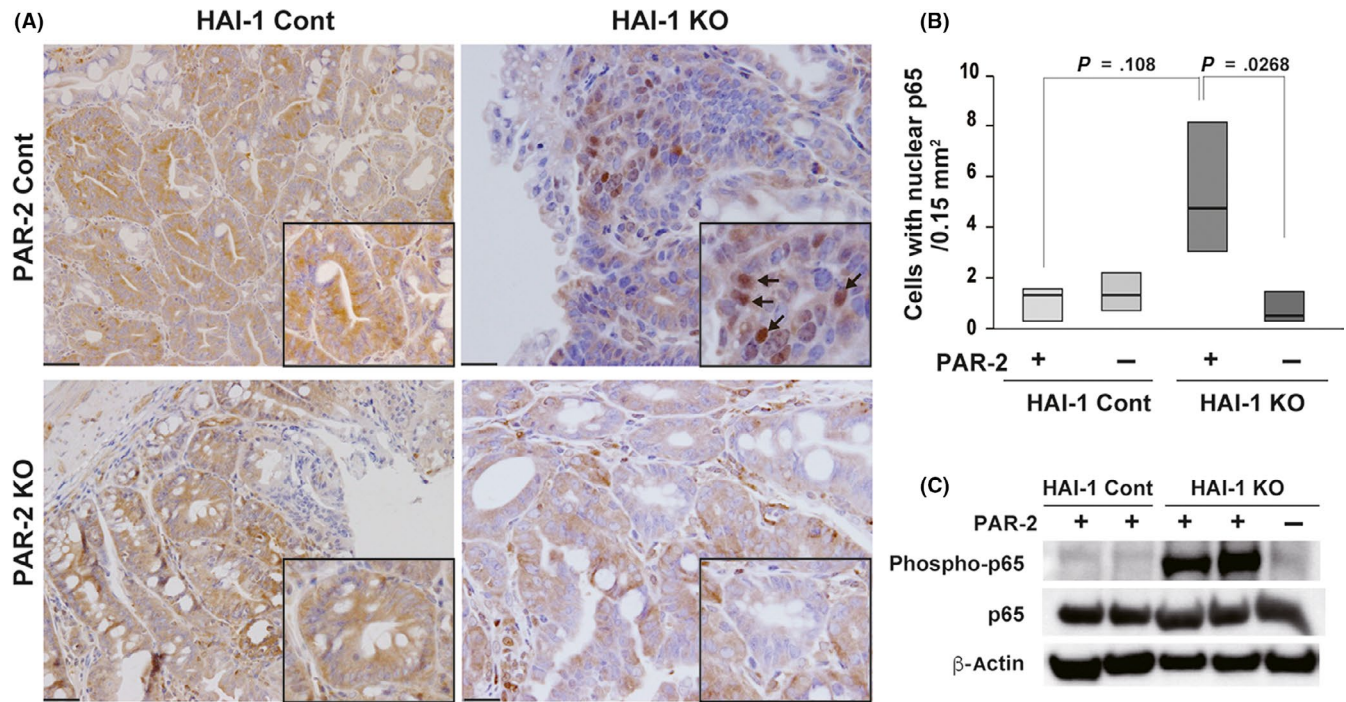


**FIGURE 3** Nuclear factor- $\kappa$ B (NF- $\kappa$ B) activation was decreased by the absence of protease-activated receptor-2 (PAR-2) in the intestines of *Spint1*-deficient *Apc*<sup>Min/+</sup> mice. A, Representative photographs of RelA/p65 nuclear translocation in intestinal tumor cells (arrows). Higher magnification images are also shown with indication of RelA/p65-positive nuclei by arrows (inset). Bar = 50  $\mu$ m. B, Quantitation of nuclear RelA/p65-positive cells from *Spint1*<sup>LoxP/LoxP</sup>/*Apc*<sup>Min/+</sup> mice (hepatocyte growth factor activator inhibitor-1 [HAI-1] control [cont] + PAR-2 cont) (n = 4), *Spint1*<sup>LoxP/LoxP</sup>/*F2r1*<sup>-/-</sup>/*Apc*<sup>Min/+</sup> mice (HAI-1 cont + PAR-2 knockout [KO]) (n = 4), *Spint1*<sup>LoxP/LoxP</sup>/*Villin-Cre*/*Apc*<sup>Min/+</sup> mice (HAI-1 KO + PAR-2 cont) (n = 4), and *Spint1*<sup>LoxP/LoxP</sup>/*Villin-Cre*/*F2r1*<sup>-/-</sup>/*Apc*<sup>Min/+</sup> mice (HAI-1 KO + PAR-2 KO) (n = 4) at 15 weeks of age. Box shows interquartile range. Median is indicated by a bold line. C, Immunoblot analysis for the effect of *Spint1* deletion (HAI-1 KO) or *Spint1*/*F2r1* double deletions (HAI-1 KO/PAR2 -) on the phosphorylation (Phospho-) of RelA/p65 in the intestinal tumor tissues

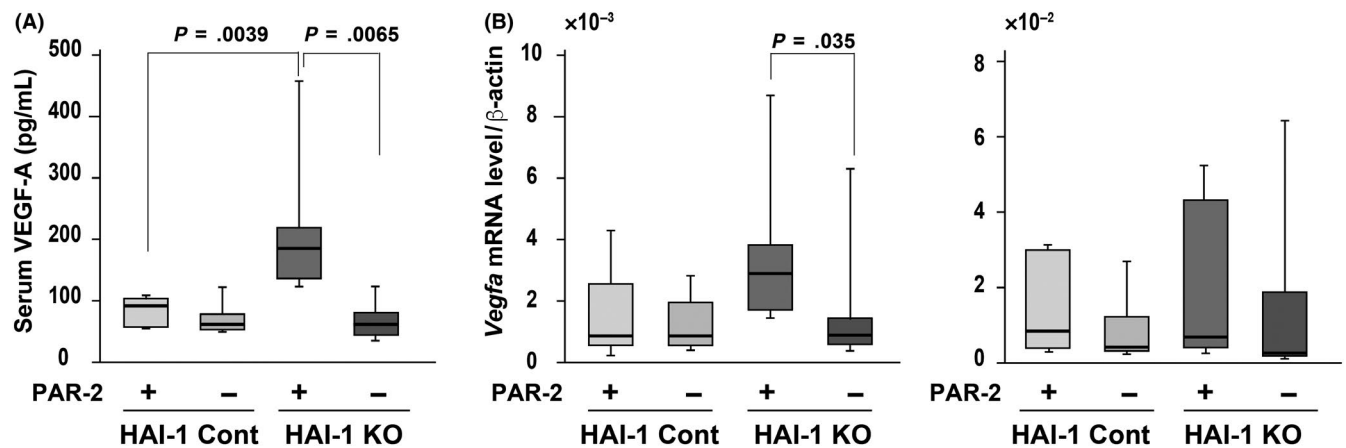
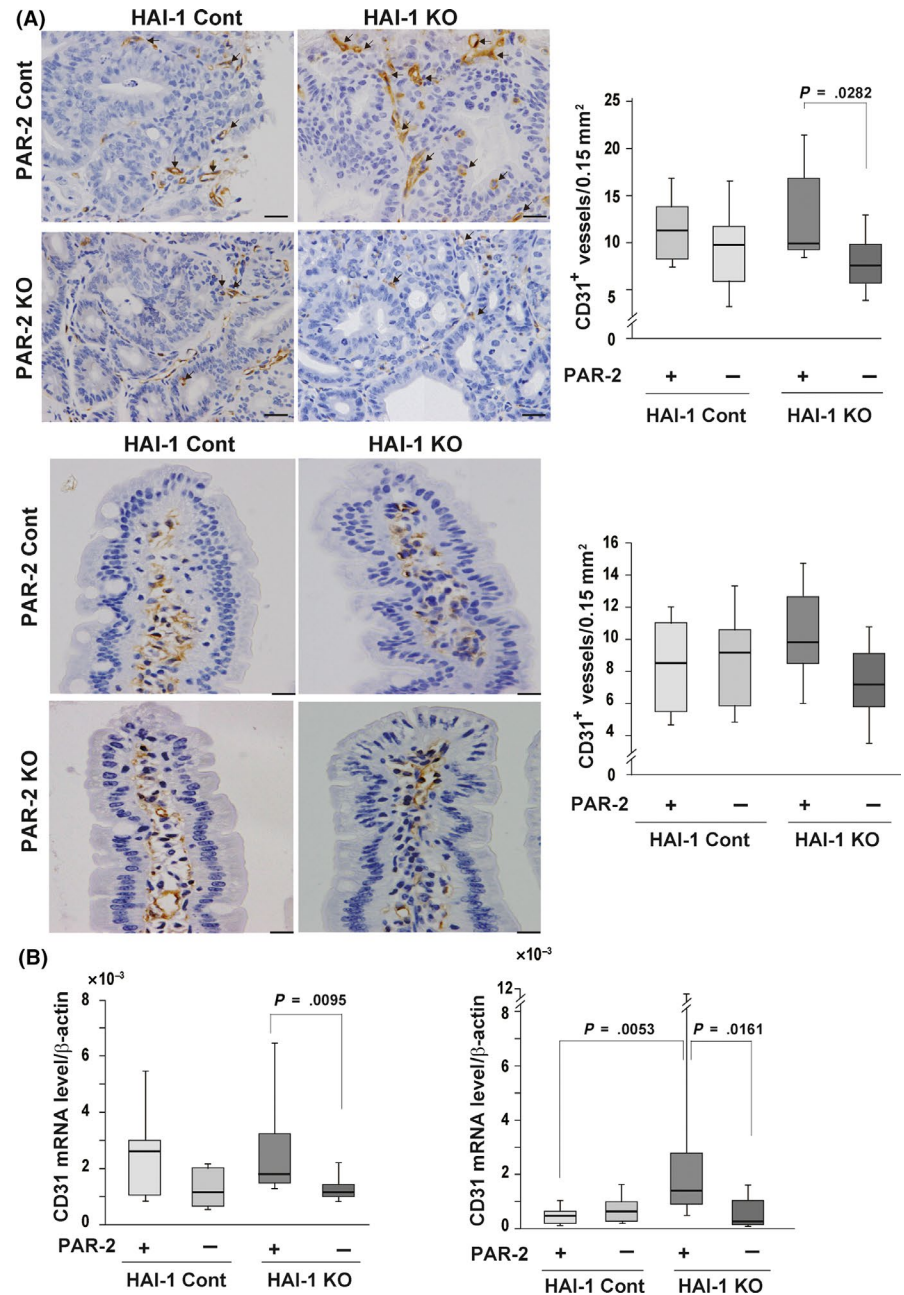


**FIGURE 4** Vascular endothelial growth factor-A (VEGF-A) levels in the intestinal tissues and sera of mice. A, ELISA measurements of VEGF-A in sera from each group. B, Quantitative RT-PCR for *Vegfa* mRNA levels in tumor (left panel) and nontumor mucosa tissues (right panel) from *Spint1*<sup>LoxP/LoxP</sup>/*Apc*<sup>Min/+</sup> mice (hepatocyte growth factor activator inhibitor-1 [HAI-1] control [cont] + PAR-2 cont) (n = 7), *Spint1*<sup>LoxP/LoxP</sup>/*F2r1*<sup>-/-</sup>/*Apc*<sup>Min/+</sup> mice (HAI-1 cont + PAR-2 knockout [KO]) (n = 7), *Spint1*<sup>LoxP/LoxP</sup>/*Villin-Cre*/*Apc*<sup>Min/+</sup> mice (HAI-1 KO + PAR-2 cont) (n = 7), and *Spint1*<sup>LoxP/LoxP</sup>/*Villin-Cre*/*F2r1*<sup>-/-</sup>/*Apc*<sup>Min/+</sup> mice (HAI-1 KO + PAR-2 KO) (n = 7). Box and whiskers indicate the interquartile range and sample maxima and minima, respectively. Median is indicated by a bold line

*Villin-Cre*/*F2r1*<sup>-/-</sup>/*Apc*<sup>Min/+</sup> mice was larger than that of *Spint1*<sup>LoxP/LoxP</sup>/*F2r1*<sup>-/-</sup>/*Apc*<sup>Min/+</sup> mice, but the serum VEGF-A levels and VEGFA mRNA levels were similar between these 2 groups. Thus, the increased serum VEGF-A proteins did not simply rely on the secondary effect

of increased tumor burden. As PAR-2 activation in fact enhanced the VEGFA mRNA levels in Caco2 cells, we hypothesized that both factors (increased tumor burden and HAI-1 deficiency-induced PAR-2 activation) account for the enhanced VEGF-A production in *Spint1*<sup>LoxP/LoxP</sup>

**FIGURE 5** Effect of protease-activated receptor-2 (PAR-2) deficiency on capillary density. A, Immunohistochemical analyses of CD31. Representative photographs of CD31<sup>+</sup> vessels (arrows) (left panel), quantitation of CD31<sup>+</sup> vessels (right panel) of tumor tissues (upper panel), and nontumor mucosa tissues (lower panel) from *Spint1*<sup>LoxP/LoxP</sup>/*Apc*<sup>Min/+</sup> mice (hepatocyte growth factor activator inhibitor-1 [HAI-1] control [cont] + PAR-2 cont) (n = 7), *Spint1*<sup>LoxP/LoxP</sup>/*F2r1*<sup>-/-</sup>/*Apc*<sup>Min/+</sup> mice (HAI-1 cont + PAR-2 knockout [KO]) (n = 6), *Spint1*<sup>LoxP/LoxP</sup>/*Villin-Cre/Apc*<sup>Min/+</sup> mice (HAI-1 KO + PAR-2 cont) (n = 5), and *Spint1*<sup>LoxP/LoxP</sup>/*Villin-Cre/F2r1*<sup>-/-</sup>/*Apc*<sup>Min/+</sup> mice (HAI-1 KO + PAR-2 KO) (n = 5). Bar = 20  $\mu$ m. B, Quantitative RT-PCR for *Pecam1* (CD31) mRNA expression in tumor (left panel) and nontumor mucosa (right panel) tissues. Box and whiskers indicate the interquartile range and sample maxima and minima, respectively. Median is indicated by a bold line



*Villin-Cre/Apc*<sup>Min/+</sup> mice. Importantly, nuclear translocation of  $\beta$ -catenin and activation of the hepatocyte growth factor-MET axis, which were enhanced in *Spint1*-deleted *Apc*<sup>Min/+</sup> mice,<sup>5</sup> were not significantly altered by compound PAR-2/*F2r1* deletion (Figure S4).

Nuclear factor- $\kappa$ B signaling has important roles in cancer progression, primarily through its stimulation of cell proliferation, survival, and angiogenesis.<sup>32-34</sup> In this regard, activation of PAR-2 by an extracellular trypsin-like serine protease transduces NF- $\kappa$ B signaling.<sup>22,29,35</sup> Although several in vitro studies have reported that PAR-2 promotes the proliferation of human colon cancer cell lines,<sup>36-38</sup> the role of PAR-2 in colorectal cancer has not been addressed in vivo. Here, we report for the first time that PAR-2 promotes tumor formation and growth in mouse intestine harboring the *Apc* mutation. Protease-activated receptor-2 is expressed not only in epithelial cells

but also leukocytes, endothelial cells, and smooth muscle cells.<sup>19,39,40</sup> Although PAR-2 is hardly detectable in normal fibroblasts, activated fibroblasts express PAR-2, as do cancer-associated fibroblasts.<sup>28,41</sup> Protease-activated receptor-2 is also expressed by most cancer cells of epithelial origin, including colorectal cancer cells.<sup>42</sup> In this study, we did not address which cells were responsible for PAR-2-induced tumor promotion and VEGF-A expression. In a mouse model of matrilysin-induced skin carcinogenesis, the excess activation of keratinocyte PAR-2 was crucial for tumor promotion.<sup>25</sup> As HAI-1 and TTSP are both membrane anchored with mostly local actions, it is likely that epithelial PAR-2 of the intestine is also responsible for the increased frequency of tumor formation in the current study. To clarify this question, further studies using mice with intestinal epithelium-specific *F2r1*-deletion will be required.

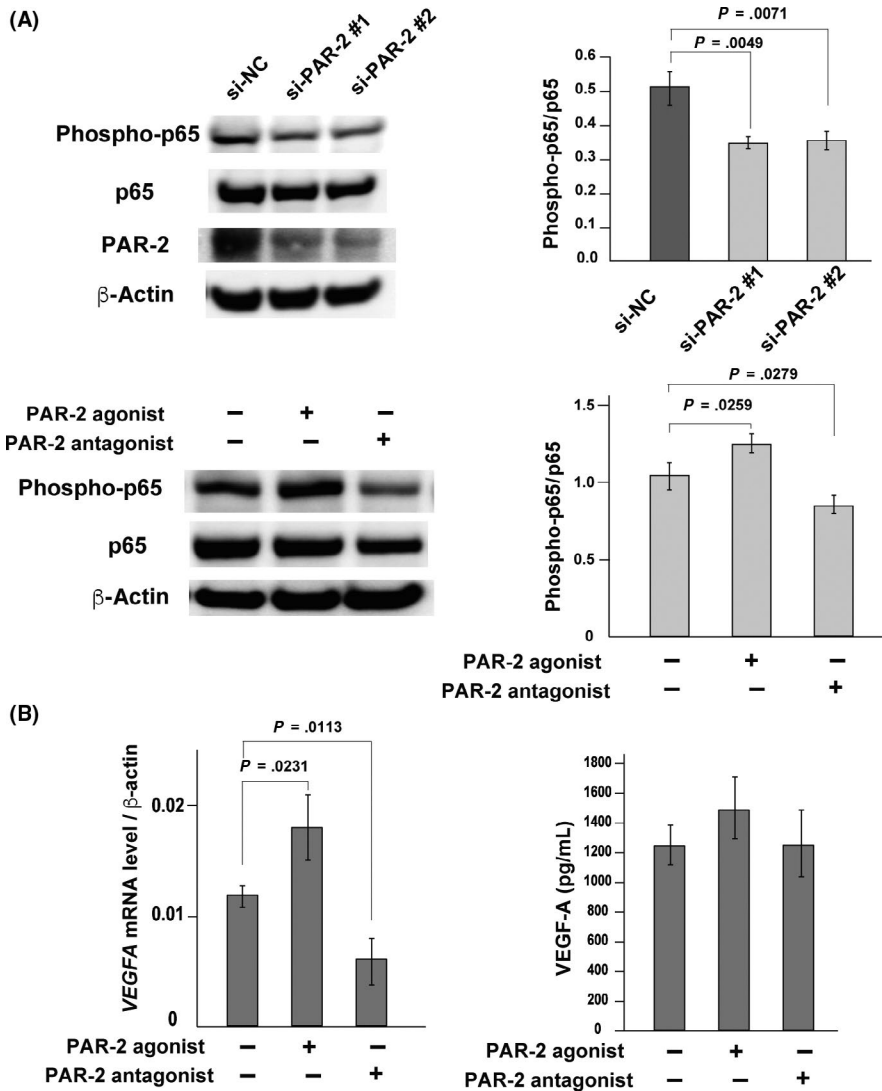


**FIGURE 6** Protease-activated receptor-2 (PAR-2) activated nuclear factor- $\kappa$ B (NF- $\kappa$ B) signaling and induced the expression of vascular endothelial growth factor-A (VEGF-A) in Caco2 colon cancer cell line. A, Immunoblot analysis of phosphorylated (Phospho-)p65 and total p65. Caco2 cells were treated with 2 kinds of *F2RL1* siRNAs: PAR-2 siRNA #1 (si-PAR-2 #1) and PAR-2 siRNA#2 (si-PAR-2 #2). Control siRNA (si-NC)-treated cells were also analyzed (upper panel). Effects of PAR-2 agonist (10  $\mu$ mol/L) and antagonist (10  $\mu$ mol/L) on Caco2 cells (lower panel). Ratio of phospho-p65 to p65 of each group is shown in the right panels. Error bar, SD of 3 independent experiments. B, Quantitative RT-PCR for VEGF-A mRNA levels in Caco2 cells treated with PAR-2 agonist (10  $\mu$ mol/L) or antagonist (10  $\mu$ mol/L) (left panel) and ELISA measurements of VEGF-A in the culture supernatant of Caco2 cells (right panel). Error bar, SD of 3 independent experiments

This study did not identify the protease(s) responsible for the presumed excess activation of PAR-2 in the *Spint1*-deleted *Apc*<sup>Min/+</sup> intestine. Protease-activated receptor-2 is activated by various trypsin-like serine proteases.<sup>14-22</sup> Among them, the main candidate protease is matriptase, a HAI-1 regulated protease that is widely expressed in epithelial cells, including enterocytes.<sup>2,43</sup> The matriptase-PAR-2 axis has been implicated in development, inflammation, and cancer.<sup>23,25,44-46</sup> The *ST14* gene, encoding matriptase, was originally proposed as a suppressor of colon cancer.<sup>47</sup> Indeed, ablation of *St14*/matriptase in the intestinal epithelium impaired the barrier function and induced mucosal inflammation, eventually resulting in the formation of colon adenocarcinoma in mice.<sup>48</sup> Excess matriptase activity also leads to the disturbance of epithelial integrity in the intestine.<sup>49,50</sup> Moreover, matriptase is known to be upregulated in various human cancers and deregulated activities of matriptase contribute to tumor progression.<sup>51-53</sup> In colorectal cancers, the ratio of matriptase / HAI-1 mRNA is increased during the early stages of carcinogenesis.<sup>8</sup> These lines of evidence indicate that normal, tightly regulated matriptase activity is critically required for the integrity of intestinal epithelium, and dysregulation of matriptase contributes to neoplastic progression of

the intestinal epithelium. Protease-activated receptor-2 can also be activated by the tissue factor (TF)/factor VIIa (FVIIa) complex, coagulation factor Xa (FXa), and the ternary TF/FVIIa/FXa complex.<sup>19,54,55</sup> Like matriptase and PAR-2, TF is frequently expressed in various cancers, including colorectal cancer.<sup>54,56</sup> A recent study reported that TF-dependent coagulation initiation on epithelia triggers matriptase activation, which in turn activates PAR-2, suggesting that cancer-associated loss of vascular integrity might trigger TTSP activation secondary to activation of the coagulation cascade.<sup>57</sup> In a previous study of TF expression in human colorectal carcinoma cell lines, most lines expressed TF with augmented expression in a highly metastatic subline.<sup>58</sup> In colorectal cancers, high TF expression in tumor cells also correlated with poor patient prognosis.<sup>59,60</sup> Kallikrein-related peptidases (KLKs) are also candidate PAR-2 activators in this context.<sup>61</sup> Matriptase is an activator of KLK5, which is also directly inhibited by HAI-1.<sup>62-64</sup> Kallikrein-related peptidase 5 is trypsin-like serine proteinase that can efficiently activate PAR-2 as well as KLK14, another PAR-2 activating KLK.<sup>65</sup> Kallikrein-related peptidase 7 is known to be expressed by human colon cancer cell lines in vitro and colon cancer tissues in vivo.<sup>14,61</sup>



In summary, we showed that a protease-activated G-protein-coupled receptor, PAR-2, contributes to intestinal carcinogenesis in the murine *Apc<sup>Min</sup>* model, and accounts, at least partly, for the increased tumor susceptibility associated with genetically induced deficiency of the TTSP inhibitor HAI-1 in intestinal epithelial cells. Mechanistically, PAR2 signaling promotes NF- $\kappa$ B activation and tumor angiogenesis. This study illustrates the importance of tight regulation of pericellular serine protease activities for epithelial homeostasis and points to serine proteases and protease-activated receptors as therapeutic targets in epithelial carcinogenesis.

## ACKNOWLEDGMENTS

We thank Ms Yukari Torisu and Junko Kurogi for their excellent technical assistance. This work was supported by Japan Society for the Promotion of Science KAKENHI 15K08311 (MK), 16H05175 (HK), and 17K08764 (TF) and by the French National Research Agency (ANR-15-CE14-0009; EC).

## DISCLOSURE

The authors declare that there is no conflict of interest.

## ORCID

Makiko Kawaguchi  <https://orcid.org/0000-0001-8210-5460>

Hiroaki Kataoka  <https://orcid.org/0000-0001-9948-0451>

Tsuyoshi Fukushima  <https://orcid.org/0000-0002-9350-777X>

## REFERENCES

- Kataoka H, Suganuma T, Shimomura T, et al. Distribution of hepatocyte growth factor activator inhibitor type 1 (HAI-1) in human tissues. Cellular surface localization of HAI-1 in simple columnar epithelium and its modulated expression in injured and regenerative tissues. *J Histochem Cytochem*. 1999;47(5):673-682.
- Kataoka H, Kawaguchi M, Fukushima T, Shimomura T. Hepatocyte growth factor activator inhibitors (HAI-1 and HAI-2): emerging key players in epithelial integrity and cancer. *Pathol Int*. 2018;68(3):145-158.
- Antalis TM, Bugge TH, Wu Q. Membrane-anchored serine proteases in health and disease. *Prog Mol Biol Transl Sci*. 2011;99:1-50.
- Kawaguchi M, Takeda N, Hoshiko S, et al. Membrane-bound serine protease inhibitor HAI-1 is required for maintenance of intestinal epithelial integrity. *Am J Pathol*. 2011;179(4):1815-1826.
- Hoshiko S, Kawaguchi M, Fukushima T, et al. Hepatocyte growth factor activator inhibitor type 1 is a suppressor of intestinal tumorigenesis. *Cancer Res*. 2013;73(8):2659-2670.
- Nagaike K, Kohama K, Uchiyama S, et al. Paradoxically enhanced immunoreactivity of hepatocyte growth factor activator inhibitor type 1 (HAI-1) in cancer cells at the invasion front. *Cancer Sci*. 2004;95(9):728-735.
- Kataoka H, Hamasuna R, Itoh H, Kitamura N, Koono M. Activation of hepatocyte growth factor/scatter factor in colorectal carcinoma. *Cancer Res*. 2000;60(21):6148-6159.
- Vogel LK, Sæbø M, Skjelbred CF, et al. The ratio of Matriptase/HAI-1 mRNA is higher in colorectal cancer adenomas and carcinomas than corresponding tissue from control individuals. *BMC Cancer*. 2006;6:176.
- Kawaguchi M, Yamamoto K, Kanemaru A, et al. Inhibition of nuclear factor- $\kappa$ B signaling suppresses Spint1-deletion-induced tumor susceptibility in the *Apc<sup>Min</sup>/+* model. *Oncotarget*. 2016;7(42):68614-68622.
- Gieseler F, Ungefroren H, Settmacher U, Hollenberg MD, Kaufmann R. Proteinase-activated receptors (PARs) - focus on receptor-receptor-interactions and their physiological and pathophysiological impact. *Cell Commun Signal*. 2013;11:86.
- Ungefroren H, Witte D, Rauch B, et al. Proteinase-activated receptor 2 may drive cancer progression by facilitating TGF- $\beta$  signaling. *Int J Mol Sci*. 2017;18(11):2494.
- Lohman R-J, Cotterell AJ, Suen J, et al. Antagonism of protease-activated receptor 2 protects against experimental colitis. *J Pharmacol Exp Ther*. 2012;340(2):256-265.
- Tahara T, Shibata T, Nakamura M, et al. Promoter methylation of protease-activated receptor (PAR2) is associated with severe clinical phenotypes of ulcerative colitis (UC). *Clin Exp Med*. 2009;9(2):125-130.
- Gratio V, Lorient C, Virca GD, et al. Kallikrein-related peptidase 14 acts on proteinase-activated receptor 2 to induce signaling pathway in colon cancer cells. *Am J Pathol*. 2011;179(5):2625-2636.
- Coughlin SR. Thrombin signalling and protease-activated receptors. *Nature*. 2000;407(6801):258-264.
- Seitz I, Hess S, Schulz H, et al. Membrane-type serine protease-1/matriptase induces interleukin-6 and -8 in endothelial cells by activation of protease-activated receptor-2. *Arterioscler Thromb Vasc Biol*. 2007;27(4):769-775.
- Liu C, Li Q, Zhou X, Kolosov VP, Perelman JM. Human airway trypsin-like protease induces mucin5AC hypersecretion via a protease-activated receptor 2-mediated pathway in human airway epithelial cells. *Arch Biochem Biophys*. 2013;535(2):234-240.
- Wilson S, Greer B, Hooper J, et al. The membrane-anchored serine protease, TMPRSS2, activates PAR-2 in prostate cancer cells. *Biochem J*. 2005;388(Pt 3):967-972.
- Wojtukiewicz MZ, Hempel D, Sierko E, Tucker SC, Honn KV. Protease-activated receptors (PARs)-biology and role in cancer invasion and metastasis. *Cancer Metastasis Rev*. 2015;34(4):775-796.
- Driesbaugh KH, Buzza MS, Martin EW, Conway GD, Kao JPY, Antalis TM. Proteolytic activation of the Protease-activated Receptor (PAR)-2 by the glycosylphosphatidylinositol-anchored serine protease testisin. *J Biol Chem*. 2015;290(6):3529-3541.
- Takeuchi T, Harris JL, Huang W, Yan KW, Coughlin SR, Craik CS. Cellular localization of membrane-type serine protease 1 and identification of protease-activated receptor-2 and single-chain urokinase-type plasminogen activator as substrates. *J Biol Chem*. 2000;275(34):26333-26342.
- Pawar NR, Buzza MS, Antalis TM. Membrane-anchored serine proteases and protease-activated receptor-2-mediated signaling: co-conspirators in cancer progression. *Cancer Res*. 2019;79(2):301-310.
- Camerer E, Barker A, Duong DN, et al. Local protease signaling contributes to neural tube closure in the mouse embryo. *Dev Cell*. 2010;18(1):25-38.
- List K, Szabo R, Molinolo A, et al. Deregulated matriptase causes ras-independent multistage carcinogenesis and promotes ras-mediated malignant transformation. *Genes Dev*. 2005;19(16):1934-1950.
- Sales KU, Friis S, Konkell JE, et al. Non-hematopoietic PAR-2 is essential for matriptase-driven pre-malignant progression and potentiation of ras-mediated squamous cell carcinogenesis. *Oncogene*. 2014;34:346-356.
- Lindner JR, Kahn ML, Coughlin SR, et al. Delayed onset of inflammation in protease-activated receptor-2-deficient mice. *J Immunol*. 2000;165(11):6504-6510.
- Fukushima T, Kawaguchi M, Yamamoto K, et al. Aberrant methylation and silencing of the *SPINT2* gene in high-grade gliomas. *Cancer Sci*. 2018;109(9):2970-2979.
- Kanemaru AI, Yamamoto K, Kawaguchi M, et al. Deregulated matriptase activity in oral squamous cell carcinoma promotes the infiltration of cancer-associated fibroblasts by paracrine activation of protease-activated receptor 2. *Int J Cancer*. 2017;140(1):130-141.

29. Johnson JJ, Miller DL, Jiang R, et al. Protease Activated Receptor-2 (PAR-2)-mediated NF- $\kappa$ B activation suppresses inflammation-associated tumor suppressor MicroRNAs in oral squamous cell carcinoma. *J Biol Chem*. 2016;291(13):6936-6945.
30. Guo D, Zhou H, Wu Y, et al. Involvement of ERK1/2/NF- $\kappa$ B signal transduction pathway in TF/FVIIa/PAR2-induced proliferation and migration of colon cancer cell SW620. *Tumor Biol*. 2011;32(5):921-930.
31. Das K, Prasad R, Ansari SA, Roy A, Mukherjee A, Sen P. Matrix metalloproteinase-2: A key regulator in coagulation proteases mediated human breast cancer progression through autocrine signaling. *Biomed Pharmacother*. 2018;105:395-406.
32. Perkins ND. The diverse and complex roles of NF- $\kappa$ B subunits in cancer. *Nat Rev Cancer*. 2012;12(2):121-132.
33. Ben-Neriah Y, Karin M. Inflammation meets cancer, with NF- $\kappa$ B as the matchmaker. *Nat Immunol*. 2011;12(8):715-723.
34. Karin M. Nuclear factor-kappaB in cancer development and progression. *Nature*. 2006;441(7092):431-436.
35. Kanke T, Macfarlane SR, Seatter MJ, et al. Proteinase-activated receptor-2-mediated activation of stress-activated protein kinases and inhibitory kappa B kinases in NCTC 2544 keratinocytes. *J Biol Chem*. 2001;276(34):31657-31666.
36. Wu Y, Wang J, Zhou H, et al. Effects of calcium signaling on coagulation factor VIIa-induced proliferation and migration of the SW620 colon cancer cell line. *Mol Med Rep*. 2014;10(6):3021-3026.
37. Ma Y, Bao-Han W, Lv X, et al. MicroRNA-34a mediates the autocrine signaling of PAR2-activating proteinase and its role in colonic cancer cell proliferation. *PLoS ONE*. 2013;8(8):e72383.
38. Hu L, Xia L, Zhou H, et al. TF/FVIIa/PAR2 promotes cell proliferation and migration via PKC $\alpha$  and ERK-dependent c-Jun/AP-1 pathway in colon cancer cell line SW620. *Tumor Biol*. 2013;34(5):2573-2581.
39. Allard B, Bara I, Gilbert G, et al. Protease activated receptor-2 expression and function in asthmatic bronchial smooth muscle. *PLoS ONE*. 2014;9(2):e86945.
40. Johansson U, Lawson C, Dabare M, et al. Human peripheral blood monocytes express protease receptor-2 and respond to receptor activation by production of IL-6, IL-8, and IL-1 $\beta$ . *J Leukoc Biol*. 2005;78(4):967-975.
41. Gruber BL, Marchese MJ, Santiago-Schwarz F, Martin CA, Zhang J, Kew RR. Protease-activated receptor-2 (PAR-2) expression in human fibroblasts is regulated by growth factors and extracellular matrix. *J Invest Dermatol*. 2004;123(5):832-839.
42. Elste AP, Petersen I. Expression of proteinase-activated receptor 1-4 (PAR 1-4) in human cancer. *J Mol Histol*. 2010;41(2-3):89-99.
43. Oberst MD, Singh B, Ozdemirli M, Dickson RB, Johnson MD, Lin C-Y. Characterization of matriptase expression in normal human tissues. *J Histochem Cytochem*. 2003;51(8):1017-1025.
44. Bardou O, Menou A, François C, et al. Membrane-anchored serine protease matriptase is a trigger of pulmonary fibrogenesis. *Am J Respir Crit Care Med*. 2016;193(8):847-860.
45. Szabo R, Peters DE, Kosa P, Camerer E, Bugge TH. Regulation of fetomaternal barrier by matriptase- and PAR-2-mediated signaling is required for placental morphogenesis and mouse embryonic survival. *PLoS Genet*. 2014;10(7):e1004470.
46. Ye J, Kawaguchi M, Haruyama Y, et al. Loss of hepatocyte growth factor activator inhibitor type 1 participates in metastatic spreading of human pancreatic cancer cells in a mouse orthotopic transplantation model. *Cancer Sci*. 2014;105(1):44-51.
47. Zhang Y, Cai X, Schlegelberger B, Zheng S. Assignment of human putative tumor suppressor genes ST13 (alias SNC6) and ST14 (alias SNC19) to human chromosome bands 22q13 and 11q24 $\rightarrow$ q25 by in situ hybridization. *Cytogenet Cell Genet*. 1998;83(1-2):56-57.
48. Kosa P, Szabo R, Molinolo AA, Bugge TH. Suppression of Tumorigenicity-14, encoding matriptase, is a critical suppressor of colitis and colitis-associated colon carcinogenesis. *Oncogene*. 2012;31(32):3679-3695.
49. Kawaguchi M, Yamamoto K, Takeda N, et al. Hepatocyte growth factor activator inhibitor-2 stabilizes Epcam and maintains epithelial organization in the mouse intestine. *Commun Biol*. 2019;2(1):11.
50. Szabo R, Callies LLK, Bugge TH. Matriptase drives early-onset intestinal failure in a mouse model of congenital tufting enteropathy. *Development*. 2019;146(22):dev183392.
51. Tanabe LM, List K. The role of type II transmembrane serine protease-mediated signaling in cancer. *FEBS J*. 2017;284(10):1421-1436.
52. Webb SL, Sanders AJ, Mason MD, Jiang WG. Type II transmembrane serine protease (TTSP) deregulation in cancer. *Front Biosci*. 2011;16(2):539-552.
53. Martin CE, List K. Cell surface-anchored serine proteases in cancer progression and metastasis. *Cancer Metastasis Rev*. 2019;38(3):357-387.
54. Kasthuri RS, Taubman MB, Mackman N. Role of tissue factor in cancer. *J Clin Oncol*. 2009;27(29):4834-4838.
55. Camerer E, Huang W, Coughlin SR. Tissue factor- and factor X-dependent activation of protease-activated receptor 2 by factor VIIa. *Proc Natl Acad Sci U S A*. 2000;97(10):5255-5260.
56. Jia Z-C, Wan Y-L, Tang J-Q, et al. Tissue factor/activated factor VIIa induces matrix metalloproteinase-7 expression through activation of c-Fos via ERK1/2 and p38 MAPK signaling pathways in human colon cancer cell. *Int J Colorectal Dis*. 2012;27(4):437-445.
57. Le Gall SM, Szabo R, Lee M, et al. Matriptase activation connects tissue factor-dependent coagulation initiation to epithelial proteolysis and signaling. *Blood*. 2016;127(25):3260-3269.
58. Kataoka H, Uchino H, Asada Y, et al. Analysis of tissue factor and tissue factor pathway inhibitor expression in human colorectal carcinoma cell lines and metastatic sublines to the liver. *Int J Cancer*. 1997;72(5):878-884.
59. Lykke J, Nielsen HJ. The role of tissue factor in colorectal cancer. *Eur J Surg Oncol*. 2003;29(5):417-422.
60. Seto S-I, Onodera H, Kaido T, et al. Tissue factor expression in human colorectal carcinoma: correlation with hepatic metastasis and impact on prognosis. *Cancer*. 2000;88(2):295-301.
61. Chung H, Hamza M, Oikonomopoulou K, et al. Kallikrein-related peptidase signaling in colon carcinoma cells: targeting proteinase-activated receptors. *Biol Chem*. 2012;393(5):413-420.
62. Yoon H, Laxmikanthan G, Lee J, et al. Activation profiles and regulatory cascades of the human kallikrein-related peptidases. *J Biol Chem*. 2007;282(44):31852-31864.
63. Emami N, Diamandis EP. Human kallikrein-related peptidase 14 (KLK14) is a new activator component of the KLK proteolytic cascade. *J Biol Chem*. 2008;283(6):3031-3041.
64. Sales KU, Masedunskas A, Bey AL, et al. Matriptase initiates activation of epidermal pro-kallikrein and disease onset in a mouse model of Netherton syndrome. *Nat Genet*. 2010;42(8):676-683.
65. Briot A, Deraison C, Lacroix M, et al. Kallikrein 5 induces atopic dermatitis-like lesions through PAR2-mediated thymic stromal lymphopoietin expression in Netherton syndrome. *J Exp Med*. 2009;206(5):1135-1147.

## SUPPORTING INFORMATION

Additional supporting information may be found online in the Supporting Information section.

**How to cite this article:** Kawaguchi M, Yamamoto K, Kataoka H, et al. Protease-activated receptor-2 accelerates intestinal tumor formation through activation of nuclear factor- $\kappa$ B signaling and tumor angiogenesis in *Apc*<sup>Min/+</sup> mice. *Cancer Sci*. 2020;111:1193-1202. <https://doi.org/10.1111/cas.14335>